Kejalakshmy, N., Grattan, K. T. V. & Rahman, B. M. (2015). Investigation of the Optical Modal Properties of Al+3 Doped ZnO-Coated Au Waveguide for Gas Sensing Applications Using the Finite Element Method. IEEE Sensors Journal, 16(5), pp. 1176-1181. doi: 10.1109/JSEN.2015.2498943

Investigation of the Optical Modal Properties of Al^{+3} Doped ZnO-Coated Au Waveguide for Gas Sensing Applications Using the Finite Element Method

N. T. Kejalakshmy, Kenneth T. V. Grattan, and B. M. Azizur Rahman, *Senior Member, IEEE*

***Abstract*— The modal properties of a ZnO-coated nanosized Au waveguide have been determined and analyzed using the *H*-field-based full vectorial finite-element method. The effect of Al doping of ZnO on the modal properties of the waveguide designed has also been evaluated for its potential use in environmental monitoring.**

***Index Terms*— Optical sensors, finite element analysis, surface plasmon resonance.**

I. Introduction

METAL OXIDE has been extensively used in sensors for environmental monitoring [1] and among these zinc oxide has particularly attracted considerable attention for areas such as biological sensing [2], solar cells [3], lasers [4], [5], UV detectors [6] and photo-catalysis [7]. Similarly gold nanoparticles such as wires, rods, cubes and plates have also received considerable attention due to their unique catalytic, electrical, optical, biological and other properties since the emergence of nanoscience [8] and the technology developed has allowed the exploitation of their plasmonic properties at visible wavelengths. By exploiting ZnO/Au-interface enhanced physical phenomena in the field of photocatalysis [9], applications of Raman scattering [10] and luminescence [11] have also been reported.

In this article, an Au-nanocore waveguide with an Al^{+3} doped ZnO (AZO) cladding has been designed and investigated by using the finite element method (FEM) and following that its potential for use as an optical gas sensor is reported. This paper is organized as follows. Initially details of the methodology of the FEM and the modal properties of a fundamental surface plasmonic TM mode in a ZnO/Au/ZnO one dimensional waveguide are presented. This provides a background to better understand the effects of the carrier concentration on the fundamental TM mode. Following that, an Au rectangular core with an AZO (infinite and finite) cladding is analyzed. This leads to the design of the proposed AZO-coated Au-waveguide as an environmental.

Manuscript received March 10, 2015; revised October 20, 2015; accepted October 23, 2015. Date of publication November 19, 2015; date of current version February 4, 2016. The associate editor coordinating the review of this paper and approving it for publication was Dr. Sillas Hadjiloucas.

The authors are with the School of Mathematics, Computer Science and Engineering, City University London, London EC1V 0HB, U.K. (e-mail: kejukl@yahoo.com; k.t.v.grattan@city.ac.uk; b.m.a.rahman@city.ac.uk).

Digital Object Identifier 10.1109/JSEN.2015.2498943

A full-vectorial Finite Element Method is used in this paper to obtain the modal solutions of an Au rectangular core nanowire. The FEM, based on the vector-**H**-Field formulation, has been established as one of the most accurate and numerically efficient approaches to obtaining the modal field profiles and propagation constants of the fundamental and higher-order quasi-TE and TM modes. The full-vectorial formulation is based on the minimization of the following function in terms of the nodal values of the full **H**-field vector [12],

$$\omega^2 = \frac{\int \left[(\nabla \times \mathbf{H})^* \cdot \varepsilon^{-1} (\nabla \times \mathbf{H}) + p (\nabla \cdot \mathbf{H})^* (\nabla \cdot \mathbf{H}) \right] dx dy}{\int \mathbf{H}^* \cdot \mu \mathbf{H} \, dx dy} \tag{1}$$

where **H** is the full vectorial magnetic field, * denotes the complex conjugate and transpose, ω^2 is the eigenvalue where ω is the angular frequency of the wave and ε and μ are the permittivity and permeability, respectively. The penalty function approach has also been incorporated to impose a divergence-free condition of the magnetic field to reduce the appearance of spurious modes and p is the dimensionless penalty parameter. The full vectorial FEM gives access to a number of key design parameters, thus allowing the flexibility of considering the finite dimensions of the Au core, the finite thickness of the cladding and the depletion layers, as discussed later in this paper.

In the numerical simulation, the wavelength-dependent refractive index of the gold given by Etchegoin *et al.* [13] and that of ZnO given by Jellison and Boatner [14] are taken into account. When ZnO is doped with Al^+ with the introduction of Al_2O_3, the smaller concentration of Al^+ results in an effective replacement of Zn by Al atoms and hence this increases the conductivity of the doped ZnO [15]. The corresponding modification of the plasmonic frequency has been incorporated into the optical properties of ZnO by inclusion of the resistivity [15] of AZO thin films into a Lorentz-Drude model [16] as follows.

$$\varepsilon_\omega = \varepsilon_{ZnO} - \frac{\omega_p^2}{\omega_p^2 + j\gamma\omega} \tag{2}$$

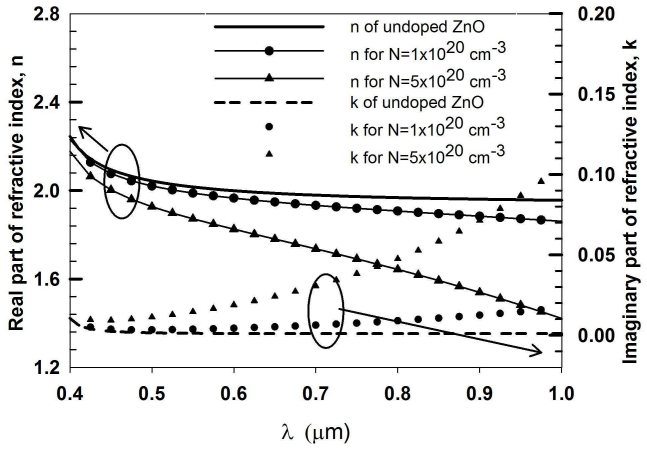

Fig. 1. Variation of the real and imaginary refractive indices with the wavelength for ZnO and AZO.

where ε_{ZnO} is the optical dielectric constant of ZnO and the second term describes the contribution of the free electrons or plasmon. In the above expression, ε_{ZnO} has the contribution arising from the UV absorption edge [14] and that of the high frequency dielectric constant. The plasma frequency, ω_p, is given by $\omega_p = \frac{Ne^2}{\varepsilon_o m^*}$ and the carrier damping constant, $\gamma = \frac{e}{\mu m^*}$. The carrier concentration, N, has been considered in the range of $1\times10^{17} < \mathrm{N} < 1\times10^{20}$ cm^{-3}. The mobility μ has been taken as 24 cm^2/Vs for the target Al^+ concentration of 2 wt.% (weight ratio) [15]. The effective mass (m*) has been taken as 0.24 times that of the mass of the electron [17]. Figure 1 shows the calculated real and imaginary parts of refractive index of the ZnO and those of AZO with carrier concentrations N=1×10^{20}cm^{-3} and 5×10^{20} cm^{-3}. It can be seen that the refractive index of ZnO is nearly 2.0 for visible wavelengths and tends to rise while approaching the UV direct band edge of ZnO at 3.3 eV [14] as shown in Fig. 1. It can be seen that an increase in the carrier concentration reduces the refractive index of ZnO and the decrement is greater for longer wavelengths. This is also associated with an increase in the imaginary part of the refractive index due the increase in the conductivity of the material. It can be also noticed that the loss is higher for longer wavelengths and also for higher levels of doping.

II. Result

To study the characteristics of the device initially an Au core sandwiched between ZnO cladding has been considered as shown in Fig.2(a) and the effect of doping on its modal characteristics has been studied. Later an Au core with Al^+ doped ZnO cladding has been considered as shown in Fig 2(b) and the change in its optical modal properties while exposing the waveguide into an oxidising agent has been analysed. The results are reported as follow.

A. Au Slab With ZnO Cladding

Initially a gold thin film sandwiched between a ZnO cladding has been investigated, using the finite element method as shown in Fig. 2(a). The waveguide is considered to be

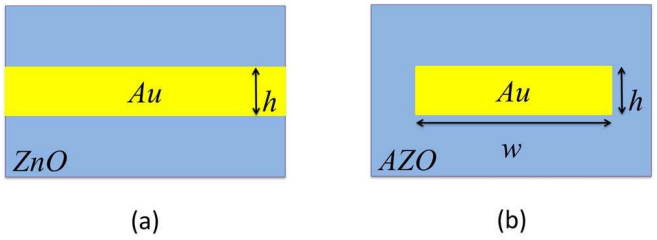

Fig. 2. Structure of Au/ZnO waveguide (a) Au sandwiched between ZnO cladding (b) Au rectangular waveguide with doped ZnO cladding.

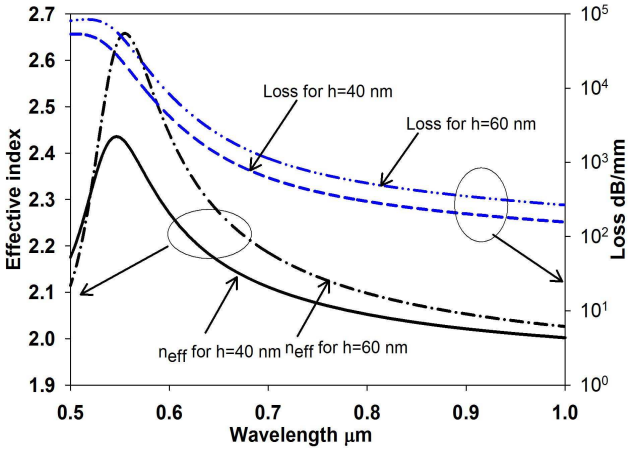

Fig. 3. Variation of the effective indices and the loss values of the fundamental even TM mode with respect to the operating wavelength for gold thickness, h=40 and 60 nm.

uniform along the horizontal X axis and also along the Z axis which serves as the direction of propagation of the light, while the interfaces are considered to be perpendicular to the Y axis. Figure 3 shows the variation of the effective indices and of the loss values of the fundamental, even TM mode (the H_x field is the even function of the y co-ordinate), which is also known as the long range plasmonic mode, for two different thicknesses of the Au core, with h=40 and 60 nm at the operating wavelength. In Figure 3, it can be observed that the effective index of the TM mode increases as the operating wavelength approaches 540 nm. Around this wavelength, the modulus of the sum of the dielectric constants ($\varepsilon_{\mathrm{ZnO}} + \varepsilon_{\mathrm{Au}}$) approaches zero, representing the limiting wavelength, λ_{sp}, to achieve the higher propagation constants in the ZnO/Au/ZnO multilayer systems [18]. Furthermore, Fig. 3 shows that the effective index and the modal loss reduce with decreasing height of the core, which is the characteristic of the coupled even TM mode, which is in turn due to the fact that as the height of the core decreases, the confinement of the mode to the metal also decreases [18].

Next, the effect of the carrier concentration on the modal property of the fundamental TM mode is considered. As a practical waveguide needs to have a core with a finite width, the Au rectangular core with height=50 nm and width=250 nm and with an AZO cladding has been considered. When the carrier concentration, N, increases, the refractive index of doped ZnO reduces from its undoped value

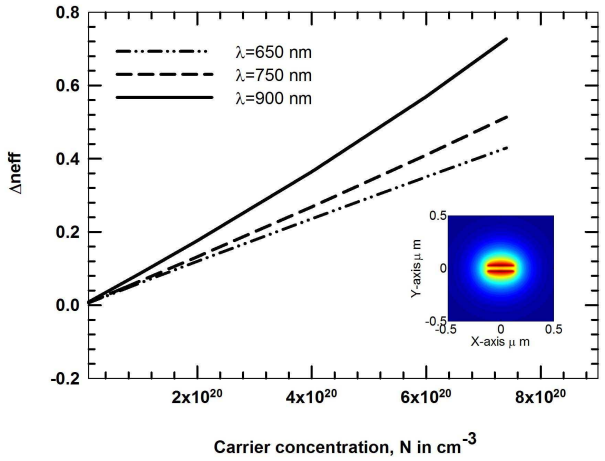

Fig. 4. Variation of the Δn_{eff} with the carrier concentration for three different λ.

and as a result, the effective index, n_{eff}, of the quasi-TM mode decreases. As N also increases, the material loss also increases due to the increasing conductivity. To evaluate these effects, the change in the effective index and the differential loss have been defined as follows;

$$\Delta n_{eff} = |n_{eff}(N_L) - n_{eff}(N)| \quad (3)$$

$$\Delta Loss = |Loss(N_L) - Loss(N)| \text{ in dB/mm} \quad (4)$$

where N_L is fixed at 1×10^{17} cm^{-3} and N is the variable carrier concentration. It can be seen from Figure 4 that Δn_{eff} increases linearly for $10^{20} < N < 10^{21}$ cm^{-3}. It can also be noted that Δn_{eff} is higher for the longer wavelengths. This agrees with the fact that the change in the refractive index of AZO is larger for longer wavelengths.

Figure 5 shows the corresponding differential modal loss. It can be observed that for longer wavelengths, where $\lambda = 900$ nm, ΔLoss increases slowly with carrier concentration and then above $N=10^{20}cm^{-3}$ it increases exponentially. This correlates well with the change in the imaginary part of the refractive index of AZO with the carrier concentration. On the other hand, for lower wavelengths, where $\lambda = 650$ nm, the differential loss, ΔLoss, does not increase much with the carrier concentration, as the imaginary part of the refractive index of AZO remains small, even when the carrier concentration is high. Furthermore for lower carrier concentrations, the confinement factor (the percentage of the modal power) inside the metal is around $\Gamma_m \approx 10\%$ at $\lambda = 650$ nm and it decreases with increasing carrier concentration. As a result, the modal loss initially decreases slightly with increasing N, until the carrier concentration reaches a value of $4 \times 10^{20} cm^{-3}$. With the further a increase in N, the modal loss increases slightly with the increasing carrier concentration.

In order to optimize the performance by involving the fundamental quasi-TM mode, the effect of the width of the core has to be considered, with respect to the modal loss. This is due to the fact that when the width is comparable to the wavelength, the variation of H_z along the X axis contributes to the E_y field. Figure 6 shows the variation of propagation length, $L_p = 1/2\beta_i$ (where β_i is the imaginary part of the propagation constant) with respect to the width for

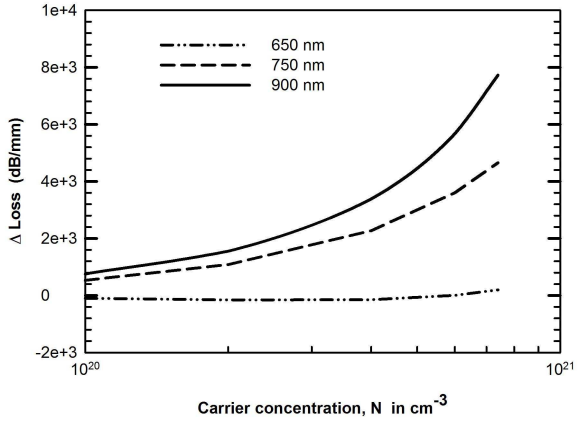

Fig. 5. The variation of ΔLoss with the carrier concentration for three different λ.

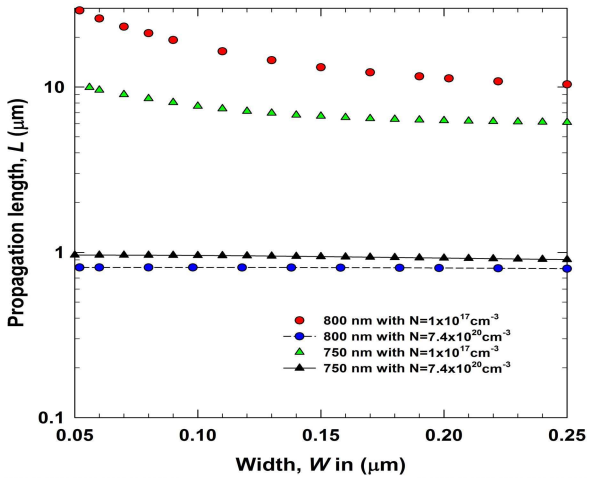

Fig. 6. Variations of the propagation length L_p with the width for different N and λ values.

two different wavelengths. It can be observed that at higher carrier concentrations, the modal loss becomes larger and as a result L_p is smaller. Furthermore, it can be seen that at lower widths, the change in L_p can be exploited as a measurement in the change of carrier concentration. This is due to the reason that a higher proportion of field is leaking into the AZO cladding when the width of the core is reduced.

In figure 6, it can also be noted that the propagation length is higher for $\lambda = 800$ nm for carrier a concentration as low as $N=1\times10^{-17}cm^{-3}$. In contrast, at a higher carrier concentration ($N=1\times10^{-20}cm^{-3}$) the propagation length is lower for $\lambda = 800$ nm. This correlates with the higher change in loss observed for longer wavelength as shown in Fig. 5. This means the propagation length is sensitive to carrier concentration provided a smaller core width (W<250 nm) is employed along with an operating wavelength whose value is far away from that of the plasmonic wavelength of the core.

B. Au Core With a Finite AZO Coating

For a practical device, the AZO cladding thickness is finite, so next a rectangular Au core with h = 60 nm and w = 250 nm and with a finite AZO coating is considered as shown

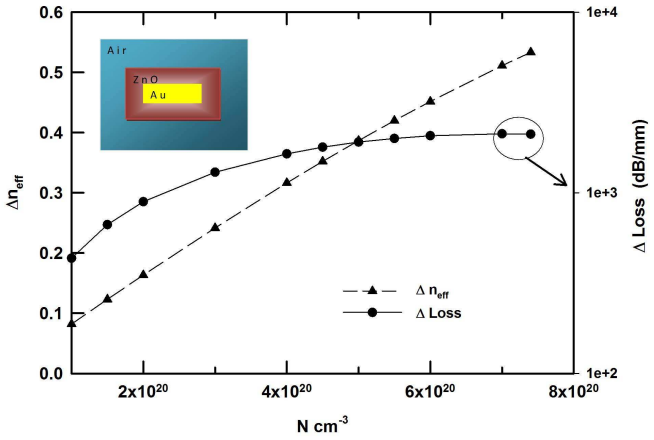

Fig. 7. Variations of Δn_{eff} and ΔLoss with the carrier concentration, N at $\lambda = 750$nm.

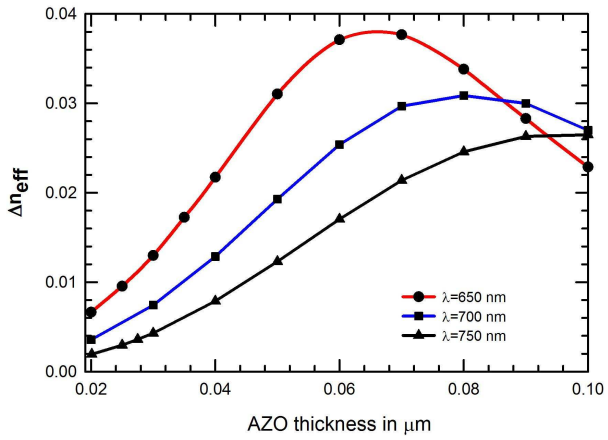

Fig. 8. Variations of Δn_{eff} with the cladding thickness.

in Figure 2(b). A 100 nm cladding of AZO around the Au core, which is in turn surrounded by an infinite air cladding, has been considered as shown in the inset of Figure 7. With only a thin, 100 nm AZO cladding and air beyond that, the equivalent index contrast of the waveguide is higher and as a result the Γ_m with the AZO/Air cladding is higher compared to that of with infinite AZO cladding, resulting in a higher loss. In the simulation, it has been observed that the propagation length of the waveguide is around 3 μm for an AZO cladding with lower carrier concentration ($N_L = 1 \times 10^{17}$cm^{-3}). As the carrier concentration increases, the refractive index of AZO decreases and as a result the power confinement (the percentage of modal power) in the AZO cladding reduces from a value of $\sim$ 80% at $N_L = 1 \times 10^{17}$cm^{-3} to a value $\sim$ 55% at N=7.4$\times 10^{20}$cm^{-3}, leaving a higher proportion of power leaking into the air cladding. Figure 7 shows the variation of Δn_{eff} and the change in ΔLoss with the carrier concentration, N. It can be seen that the refractive index changes linearly with the carrier concentration while N $> 10^{20}$cm^{-3}. Figure 7 also shows that ΔLoss increases with the carrier concentration but tends to saturate at a higher carrier concentration. This is due to the fact that at higher carrier concentration, the change in carrier concentration is accompanied by a decrease in the power confinement of the AZO cladding. In the case of infinite cladding it has been seen that at lower core width, the change in propagation length can be used to measure the change in the carrier concentration. However in the case of the finite cladding reducing the width of the core tends to reduce ΔLoss and Δn_{eff} as large amount of power leaks into the air cladding. Hence the effect of width has not been analysed.

C. Sensitivity of AZO Coated Au Core

In this section, the AZO coated Au nanocore has been analyzed in light of its potential as a gas sensor. Electrons are the majority charge carrier in an AZO material. Hence an oxidizing gas or liquid on the surface of AZO will deplete electrons, resulting in a decrease in its conductivity. The Debye thickness (length) is used to quantify the thickness of the space charge layer that has deficient carriers due to electron trapping by the chemisorbed oxidizing agent in the n-type semiconductor. The reported Debye length for AZO is in the order of 10 nm [19], for a carrier concentration of 10^{17}cm^{-3}.

In the following simulation, an Au core (core size = 250 nm $\times$ 60 nm) with an AZO coating has been considered with an initial carrier concentration of 7.4×10^{20} cm^{-3}. It has been assumed that the carrier concentration in the depletion layer (the boundary surface of AZO which is in contact with air) is depleting from a value of $N_{D,H} = 7.4 \times 10^{20}$ cm^{-3} to a value of $N_{D,L} = 10^{17}$cm^{-3} for a depth equivalent to 10 nm, the Debye length. For simplicity of the simulation, a uniform depletion of the carrier concentration has been assumed at the AZO boundary (air/AZO interface).

For a larger thickness of the cladding, the core is far away from the depletion layer. Hence the mode would not be affected to a larger degree by the change in refractive index of the depletion layer. When the cladding thickness is smaller, a higher proportion of modal power might spread into the air cladding. Hence the cladding thickness should be optimum so that a larger proportion of power resides in the depletion layer. Figure 8 shows the change in effective index with respect to the thickness of the AZO cladding for three different wavelengths.

It can be seen from Figure 8 that for a larger AZO thickness (above 90 nm), the change in effective index is larger for $\lambda = 750$ nm, compared to that for $\lambda = 650$ nm. This can be explained as follows. When the AZO thickness is larger at 100 nm, the surface plasmonic mode at $\lambda = 750$ nm has a spot-size area that is two to three times larger than that of $\lambda = 650$ nm (not shown in the Figure 8), allowing a higher proportion of the modal power inside the depletion layer, as shown in Figure 9. On the other hand, at a wavelength of 650 nm, the confinement factor is larger in the metal core compared to that in the depletion layer. Furthermore, the change in the refractive index of the depletion layer is larger for longer wavelengths. Due to these factors, the change in the modal effective index is higher for longer wavelengths, when cladding thickness is as large as 100 nm. However when the excitation wavelength lies close to the value of λ_{sp}, it is possible to achieve an enhanced change in the modal

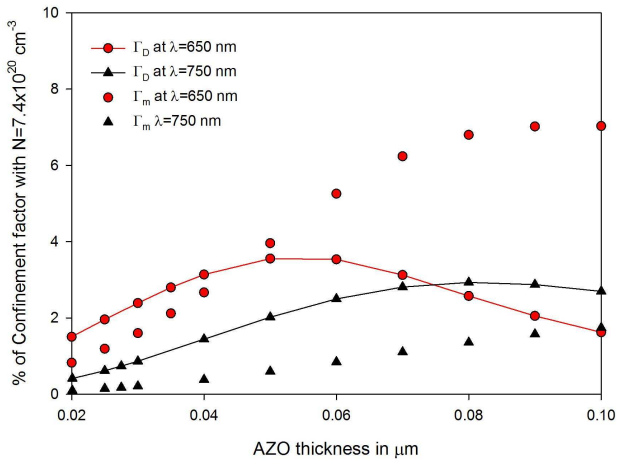

Fig. 9. Variations of the percentage of the power confinement factor in the depletion (Γ_D) and metal (Γ_m) layers with the thickness.

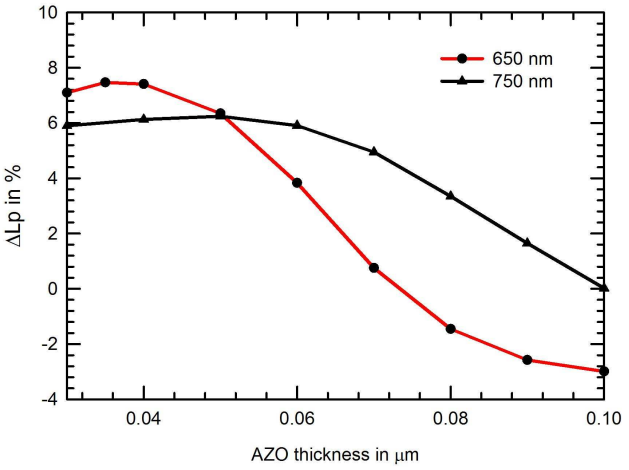

Fig. 10. Variations of the change in the propagation length with the thickness of AZO layer.

index comparable to that at the longer wavelength, using a lower cladding thickness. In Figure 8, it can be seen that when cladding thickness is lower than 80 nm, Δn_{eff} is higher at $\lambda = 650$ nm than at $\lambda = 750$ nm. This is due to the fact that the depletion layer is closer to the metal core and Γ_D becomes larger for those wavelengths that are close to λ_{sp}. This property can be exploited in designing a Mach-Zender based opto-chemical sensor [20].

Figure 10 shows the percentage of the change in the propagation length, with respect to the thickness of the AZO cladding. This is calculated as follows:

$$\Delta L_p\% = \left[1 - \frac{L_p(N_{B,L})}{L_p(N_{B,H})}\right] \times 100 \qquad (5)$$

It can be seen that as the thickness of the cladding is decreased, the change in the propagation length rises from its negative value and reaches a maximum value. Further reduction in the thickness results in leakage of a higher proportion of the power into the air cladding and as a consequence, the change in the modal loss starts to decline.

For a larger thickness, the change in propagation length is negative which means that L_p becomes higher due to depleting carrier concentration. However it can be seen that ΔL_p is a positive value for a lower cladding thickness. This can be explained as follows. With a further reduction in the cladding thickness, both the confinement factors (Γ_m and Γ_D) decreases. Furthermore Γ_m becomes comparable to that of Γ_D. So the depletion layer, which is very close to the metal core, influences the surface plasmonic mode in such a way that the modal loss increases with the increasing refractive index of the depletion layer and this effect is more pronounced for the wavelength that is closer to the λ_{sp}. Thus, in summary, the change in the modal loss is governed by the combination of carrier concentration in the depletion layer and that of the confinement factor in the metal. Furthermore an observable change in the modal loss can be achieved by choosing a suitable cladding thickness, which can be exploited in the design of a more effective intensity-based gas sensor.

III. Conclusion

The effect of the variation of the carrier concentration on the effective index of the fundamental even TM mode in an Au core/AZO cladding based plasmonic waveguide has been studied. Furthermore, the analysis has been extended for a finite coating thickness (20 nm-100 nm) of AZO on a rectangular core shaped Au core and it has been shown that the depletion of carriers for a depth equivalent to Debye thickness can cause a refractive index variation that is greater than 0.035 and a variation of the propagation length that is greater than 5%. Furthermore it has been shown that a minimum thickness of AZO coating surrounding the Au core needs to be greater than the Debye thickness. Waveguides designed and implemented according to these principles can thus find important applications in environmental monitoring systems.

References

[1] D.-D. Lee and D.-S. Lee, "Environmental gas sensors," *IEEE Sensors J.*, vol. 1, no. 3, pp. 214–224, Oct. 2001.

[2] S. A. Kumar and S.-M. Chen, "Nanostructured zinc oxide particles in chemically modified electrodes for biosensor applications," *Anal. Lett.*, vol. 41, no. 2, pp. 141–158, Feb. 2008.

[3] M. Law, L. E. Greene, J. C. Johnson, R. Saykally, and P. Yang, "Nanowire dye-sensitized solar cells," *Nature Mater.*, vol. 4, pp. 455–459, May 2005.

[4] Z. K. Tang *et al.*, "Room-temperature ultraviolet laser emission from self-assembled ZnO microcrystallite thin films," *Appl. Phys. Lett.*, vol. 72, no. 25, pp. 3270–3272, 1998.

[5] D. C. Look, D. C. Reynolds, and B. Jogai, "Optically pumped ultraviolet lasing from ZnO," *Solid State Commun.*, vol. 99, no. 12, pp. 873–875, Sep. 1996.

[6] A. Janotti and C. G. Van de Walle, "Fundamentals of zinc oxide as a semiconductor," *Rep. Prog. Phys.*, vol. 72, no. 12, p. 126501, 2009.

[7] J. Y. Lao, J. G. Wen, and Z. F. Ren, "Hierarchical ZnO nanostructures," *Nano Lett.*, vol. 2, no. 11, pp. 1287–1291, 2002.

[8] M. C. Daniel and D. Astruc, "Gold nanoparticles: Assembly, supramolecular chemistry, quantum-size-related properties, and applications toward biology, catalysis, and nanotechnology," *Chem. Rev.*, vol. 104, no. 1, pp. 293–346, 2004.

[9] C. Wang *et al.*, "Visible light plasmonic heating of Au–ZnO for the catalytic reduction of CO_2," *Nanoscale*, vol. 5, no. 15, pp. 6968–6974, 2013.

[10] A. Rumyantseva *et al.*, "Nonresonant surface-enhanced Raman scattering of ZnO quantum dots with Au and Ag nanoparticles," *ACS Nano*, vol. 7, no. 4, pp. 3420–3426, 2013.

[11] C. W. Cheng *et al.*, "Surface plasmon enhanced band edge luminescence of ZnO nanorods by capping Au nanoparticles," *Appl. Phys. Lett.*, vol. 96, no. 7, p. 071107, 2010.
[12] B. M. A. Rahman and J. B. Davies, "Penalty function improvement of waveguide solution by finite elements," *IEEE Trans. Microw. Theory Techn.*, vol. 32, no. 8, pp. 922–928, Aug. 1984.
[13] P. G. Etchegoin, E. C. Le Ru, and M. Meyer, "An analytic model for the optical properties of gold," *J. Chem. Phys.*, vol. 125, no. 16, p. 164705, 2006.
[14] G. E. Jellison and L. A. Boatner, "Optical functions of uniaxial ZnO determined by generalized ellipsometry," *Phys. Rev. B*, vol. 58, no. 7, pp. 3586–3589, Aug. 1998.
[15] C. Agashe, O. Kluth, J. Hüpkes, U. Zastrow, B. Rech, and M. Wuttig, "Efforts to improve carrier mobility in radio frequency sputtered aluminum doped zinc oxide films," *J. Appl. Phys.*, vol. 95, no. 4, pp. 1911–1917, 2004.
[16] J. Han *et al.*, "Optical and dielectric properties of ZnO tetrapod structures at terahertz frequencies," *Appl. Phys. Lett.*, vol. 89, no. 3, p. 031107, 2006.
[17] H. Morkoç, Ü. Özgür, "General properties of ZnO," in *Zinc Oxide: Fundamentals, Materials and Device Technology*. Weinheim, Germany: Wiley, 2009, p. 24.
[18] S. A. Maier, "Surface plasmon polaritons at metal/insulator interfaces," in *Plasmonics: Fundamentals and Applications*. New York, NY, USA: Springer-Verlag, 2007, pp. 21–34.
[19] Y. Chen, C. L. Zhu, and G. Xiao, "Reduced-temperature ethanol sensing characteristics of flower-like ZnO nanorods synthesized by a sonochemical method," *Nanotechnology*, vol. 17, no. 18, p. 4537, 2006.
[20] P. V. Lambeck, "Integrated opto-chemical sensors," *Sens. Actuators B, Chem.*, vol. 8, no. 1, pp. 103–116, Apr. 1992.

N. T. Kejalakshmy received the B.Sc. and M.Sc. degrees in physics from Pondicherry University, India, the M.Phil. degree from Anna University in 1997, and the Ph.D. degree from the Indian Institute of Technology Madras, India, in 2003. She joined as a Marie Curie Research Fellow to work in the Photonic Modelling Group, City University London. She is currently a Research Fellow with the School of Engineering and Mathematical Sciences, City University London. Her research interest includes electro-optics, crystal growth, numerical modeling of photonic devices, and sensors.

Kenneth T. V. Grattan was born in County Armagh, Northern Ireland, in 1953. He received the bachelor's (Hons.) degree in physics from Queen's University, Belfast, in 1974, the Ph.D. degree from Queen's University in 1978, and the D.Sc. degree from City University London, in 1992. In 1978, he became a Post-Doctoral Research Assistant with Imperial College London. He joined City University London in 1983, after five years at Imperial College, undertaking research in novel optical instrumentation, especially in fiber-optic sensor development for physical and chemical sensing. The work has led into several fields, including luminescence-based thermometry, Bragg-grating based strain sensor systems, white light interferometry, optical system modeling, and design and optical sensors for environmental and structural health monitoring. In 1983, he joined City University London, as a Lecturer in physics, being appointed Professor of Measurement and Instrumentation in 1991 and the Head of the Department of Electrical, Electronic and Information Engineering. From 2001 to 2008, he was the Associate and then the Deputy Dean of the School of Engineering, and from 2008 to 2012, the first Conjoint Dean of the School of Engineering and Mathematical Sciences and the School of Informatics. In 2013, he was appointed as the Inaugural Dean of the City Graduate School. He was Chairman of the Applied Optics Division of the U.K. Institute of Physics and the President of the Institute of Measurement and Control in 2000, and was elected a Fellow of the Royal Academy of Engineering in 2008. He received the Callendar Medal and the Honeywell Prize from the Institute of Measurement and Control.

B. M. Azizur Rahman received the B.Sc.Eng. and M.Sc.Eng. (Hons.) degrees in electrical engineering from the Bangladesh University of Engineering and Technology (BUET), Dhaka, Bangladesh, in 1976 and 1979, respectively. He also received two gold medals for being the best undergraduate and graduate student of the University in 1976 and 1979, respectively. He received the Ph.D. degree in electronic engineering from University College London, in 1982. From 1976 to 1979, he was a Lecturer with the Electrical Engineering Department, BUET. After completing the Ph.D. degree, he joined University College London as a Post-Doctoral Research Fellow and continued his research work on the finite-element modeling of optical waveguide until 1988. In 1988, he joined the Electrical, Electronic and Information Engineering Department, City University London, as a Lecturer, where he is currently a Professor. He is a member of the Institute of Engineering Technology, U.K, a Fellow of the Optical Society of America, and a Senior Member of the Institute of Electrical and Electronic Engineers, USA.